Fujii, Y. (2012), Weakness Plane Model to Simulate Effects of Stress States on Rock Strengths, True Triaxial Testing of Rocks (Proc. TTT Workshop, Beijing, Oct, 17, 2011), Kwasniewski, M., Li, X. and Takahashi, M. (Eds.), pp. 243-248, CRC Press/Balkema, Leiden, The Netherlands.

Weakness plane model to simulate effects of stress states on rock strengths

Y. Fujii
Hokkaido University, Sapporo, Japan

ABSTRACT: The "weakness plane model" was developed to simulate the effects of various stress states on the strength of rocks. The model assumes numerous planes of weakness whose directions are uniformly distributed in a rock; each plane slips or opens based on the Coulomb criterion with a tension cut-off; and the rock is regarded as failed when the ratio of the failed plane number to that of all planes reaches a certain value. The same size and strength parameters were assigned to all planes and no complicated statistical functions are used. The model has been applied to true triaxial compression, uniaxial tension, Brazilian and extension tests. The model is very simple but the effects of a stress state are simulated very well. Stress and plane failure distributions on the Schmidt net has increased the understanding of the mechanism of stress state effects on rock strength.

1 INTRODUCTION

It is well known that the strength of a rock first increases and then decreases as intermediate principal stress increases in a true triaxial test (e.g. You, 2009). This behavior would mainly be due to some effects of intermediate principal stress on microcracks; however, the mechanism of the strength behavior has not yet been well explained. Koide et al. (1986) developed a statistical model for the failure criterion of true triaxial compression based on the Griffith theory. This model can roughly approximate the effects of intermediate principal stress in true triaxial compression. However, the model is complicated and applications to other tests such as uniaxial tension, Brazilian and extension tests have not yet been shown. A simple 2-D model for simulating the effects of a stress state on rock failure was developed by Fujii & Uehara (2006). The model successfully simulated the effects of confining pressure on the axial stress value at failure in extension tests. The model was expanded to 3-D and is called the "weakness plane model" in this paper. it was applied not only to extension tests but also to true triaxial, uniaxial compression, uniaxial tension and Brazilian tests. The various effects of stress states on rock strengths will be explained based on the results of the simulations.

The objective of this research was not to precisely approximate the effects of a stress state on specific rocks as Koide et al. (1986) or You (2009) did for true triaxial tests but rather to develop a simple model and to investigate the general mechanisms of the effects of stress states on rock strengths using the model.

2 WEAKNESS PLANE MODEL

Assumptions are as follows: (1) There are numerous (20000π) planes of weakness whose directions are uniformly distributed in rock. (2) Each plane slips or opens based on the Coulomb criterion with a tension cut-off. Single values of cohesion (C), friction angle (ϕ) and tensile

strength (T_0) are assigned to all planes. (3) A rock is regarded as failed when the ratio of the failed plane number to that of all planes reaches a certain value.

Directions of 2500π normals of planes of weakness were regularly distributed on a quarter Schmidt net to assure uniform distribution so that the failure of each plane had the same weight on rock failure. The latitude ϕ and altitude θ of the normal can be calculated as

$$\phi = \tan^{-1}\left(\frac{y}{x}\right) \tag{1}$$

and

$$\theta = \frac{\pi}{2} - 2\beta\,, \tag{2}$$

where

$$\beta = \cos^{-1}\left(\frac{r}{2}\right) \tag{3}$$

and

$$r = \sqrt{x^2 + y^2}\,. \tag{4}$$

Normal and shear stresses for each plane under given principal stresses were calculated from the direction of the normal for each plane. Maximum shear stress on each plane was calculated from the shear stresses on the local coordinate. Failure of each plane was determined based on the Coulomb criterion with a tension cut-off. The number of failed planes was counted regardless of whether it had slipped or opened and the number was divided by the total plane number to obtain the failure ratio (*FR*). The rock was determined to be failed when the failure ratio reached a critical failure ratio (*FRC*).

A uniaxial compression test was simulated as an example. The cohesion of the planes of weakness was set at 10 MPa. The failure ratio increased as the axial stress increased (Fig. 1). The axial stress value at the beginning of the failure ratio increase increased as the angle of internal friction increased. The slope of the failure ratio became less steep as the friction angle increased. The increase in the slipped plane number with axial stress can be seen in Figure 2.

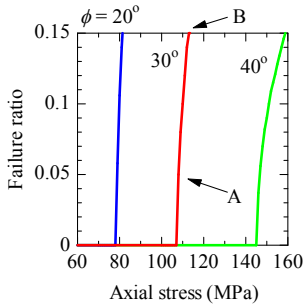

Figure 1. Simulated failure ratio using the weakness plane model. The ratio increases from certain axial stress levels according to the friction angle. The slopes of the failure ratios also depend on the friction angle.

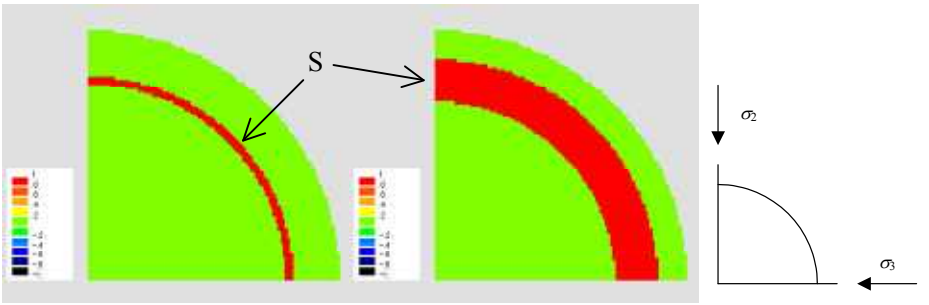

(a) Lower axial stress (b) Higher axial stress (c) Directions of principal stresses

Figure 2. Directions of failed planes in a simulated uniaxial compression test using the weakness plane model on the Schmidt net for $\phi = 30°$. Axial stress is oriented in the direction normal to the diagram. The number of slipped (S) planes increased from the lower axial stress (a), A in Figure 1, to the higher axial stress (b), B in Figure 1.

3 TRUE TRIAXIAL TEST

Typical true triaxial behavior (Fig. 3a), namely, that peak stress first increased and then decreased as intermediate stress increased was obtained from the simulation assuming base values for T_0 , C, ϕ and FRC to be 1 MPa, 10 MPa, 30° and 0.1, respectively. The effects of intermediate principal stress significantly increased as friction angle increased (Fig. 3b). Peak stress at ordinary triaxial compression was unchanged but it increased under moderate intermediate principal stress and extensional stress state as FRC increased (Fig. 3c).

Figure 4 shows the shear stress value on the planes of weakness normalized by the required shear stress for failure on the Schmidt net. The weakness planes slipped when the shear stress reached 1 as is shown in Figure 4. The donut-like distribution of the direction of the slipped plane can be observed for the case where intermediate principal stress is equal to the confining pressure (Fig. 4a). The plane failures around the direction of the intermediate principal stress were strongly restricted when a moderate intermediate principal stress was applied (Fig. 4b). The increase in strength with low-moderate intermediate principal stress was due to the restriction of the σ_1-σ_3 slips. The distribution of the direction of the slipped plane becomes a donut-like shape again under extensional stress state (Fig. 4c) but around the direction of the minimum principal stress this time. The decrease in strength under high intermediate principal stress was caused by the enhancement of the σ_2-σ_3 slips.

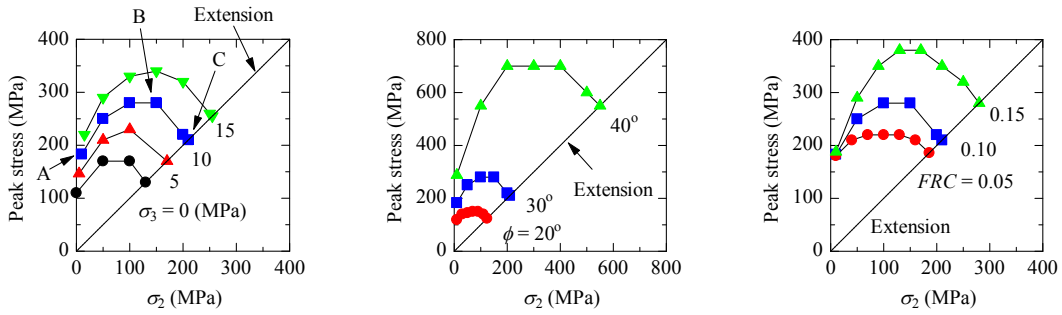

(a) Effects of σ_3 (b) Effects of ϕ (c) Effects of FRC

Figure 3. Simulated peak stress in true triaxial tests using the plane failure model. Peak stress first increases and then decreases with intermediate principal stress, which is typical true triaxial strength behavior. The effects of intermediate principal stress increase as the friction angle increases (b). Peak stress at ordinary triaxial compression is unchanged but it increases under moderate intermediate principal stress and extensional stress state as FRC increases (c).

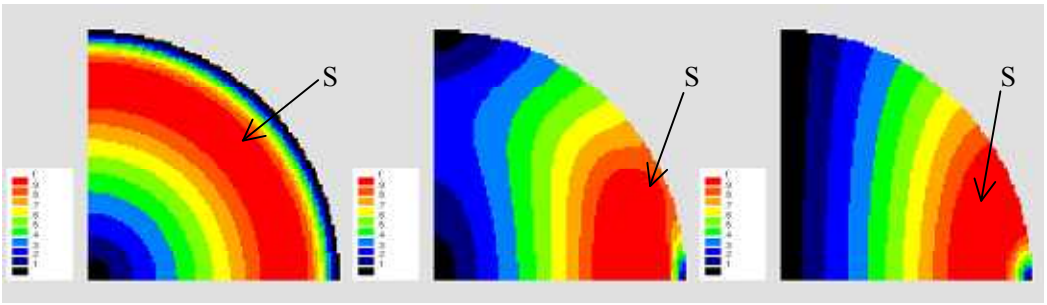

(a) Low σ_2 (A in Figure 3) (b) Moderate σ_2 (B in Figure 4) (c) Extension (C in Figure 4)

Figure 4. Shear stress value on planes of weakness normalized by the required shear stress for failure plotted on the Schmidt net. Maximum principal stress is oriented in the direction normal to the diagram. A donut-like distribution can be observed in the direction of the slipped plane for the case where intermediate principal stress was equal to the confining pressure (a). The failure around the direction of the intermediate principal stress was strongly restricted when a moderate intermediate principal stress was applied (b). Distribution of the direction of the slipped plane became a donut-like shape again under extensional stress state but around the direction of the minimum principal stress this time (c).

4 UNIAXIAL TENSION AND BRAZILIAN TESTS

Base values of T_0 , C and ϕ were assumed to be 1 MPa, 10 MPa and 30°, respectively. σ_1 and σ_2 were set at 0 for uniaxial tension. σ_2 was set at 0 and σ_1/σ_3 was kept at -3 for Brazilian test. Both strengths started from T_0 and increased as *FRC* increased. The rate of increase for the Brazilian test was larger than that for the uniaxial tension test.

It was realized from the tensile stress distribution (Fig. 6) that the compressive maximum principal stress in Brazilian tests restricted the opening of the planes whose normals were around the compressive maximum principal stress. This caused an increase in strength for the Brazilian test. The peak stress in the Brazilian test may depend on cohesion and the friction angle but they showed no variation for cohesion between 5 MPa and 15 MPa and for a friction angle between 20° and 40°.

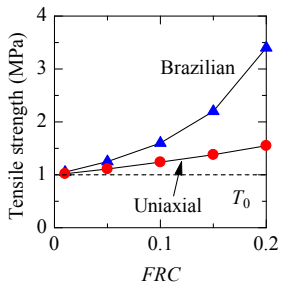

Figure 5. Simulated tensile strengths from uniaxial and Brazilian tests. Both strengths start from T_0 and increase as *FRC* increases. The rate of increase for the Brazilian test is larger than that for uniaxial tension test.

5 EXTENSION TEST

Extension tests have occasionally been carried out as an extreme stress state of true triaxial test. Strength under low confining pressure has not, however, been fully clarified although there are many studies such as Brace (1964), Mogi (1967), Tani (1996), Oikawa & Yamaguchi (2000), Ramsey & Chester (2004), Fujii & Uehara (2006), Takahashi et al. (2009), etc. Strength behavior in triaxial tension is also unknown.

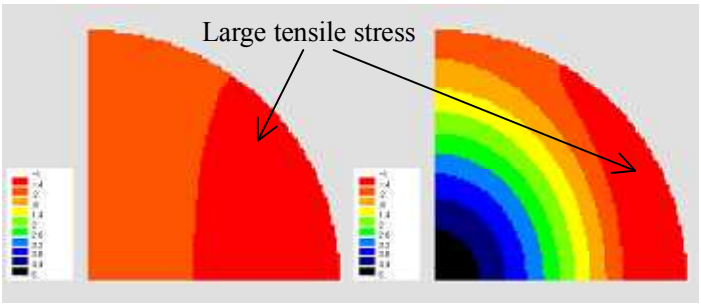

(a) Uniaxial tension (b) Brazilian test

Figure 6. Simulated tensile stress value in MPa on the Schmidt net for the uniaxial tension (a) and Brazilian tests (b). Maximum principal stress is oriented in the direction normal to the diagram. Compressive maximum principal stress in the Brazilian test restricted the opening of planes whose normals were around the compressive stress (b).

A simulation was carried out using the weakness plane model assuming base values of T_0 , C, ϕ and FRC to be 1 MPa, 10 MPa, 30° and 0.1, respectively. The peak stresses exhibited bi-linear functions (Fig. 7). The tensile strength of the rock started at the tensile strength of the weakness planes at triaxial tension (left end data of Figure 7) regardless of the values of the strength parameter. Tensile strength increased as confining pressure increased regardless of whether the confining pressure was compression or not (Region I). Plane failures were all in openings in this region (Figure 8a at A in Figure 7a). The increase in tensile strength in this region was due to a restriction of the opening of the planes caused by an increase in confining pressure. Tensile strength then began to decrease under moderate confining pressure (Region II). This was due to the beginning of plane slips (Figure 8b at B in Figure 7a). The minimum principal stress then became positive (compression) and plane failures were only by slip (Region III, Figure 8c at C in Figure 7a).

The slope of the peak stress in Regions II and III decreases as friction angle increases (Fig. 7a). Cross point of Regions I and II moves right-downward as cohesion increases (Fig. 7b). The failure criterion seems rotated clockwise as critical failure ratio increases (Fig. 7c).

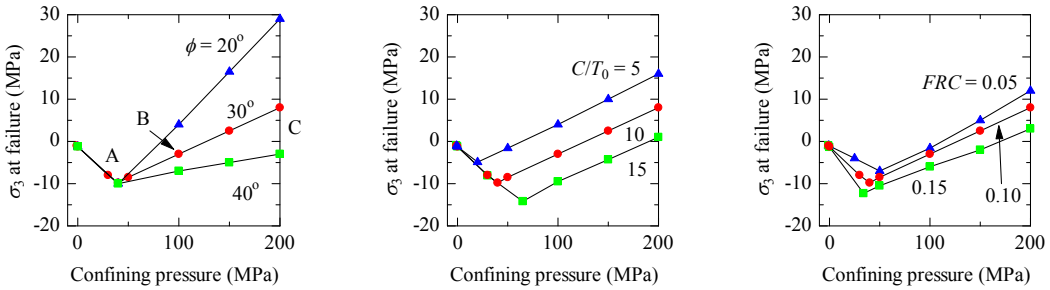

(a) Effects of ϕ (b) Effect of C/T_0 (c) Effects of FRC

Figure 7. Simulated minimum principal stress at failure in extension tests. The peak stresses exhibit bi-linear functions. The tensile strength of the specimen starts at the tensile strength of the weakness planes at triaxial tension (left end data) regardless of the values of the strength parameters. The tensile strength increases as confining pressure increases regardless of whether the confining pressure is compression or not (Region I). The tensile strength then begins to decreases under moderate confining pressure (Region II). The minimum principal stress then becomes positive (compression). The slope of the peak stress in Regions II and III decreases as the friction angle increases (a). The cross point of Regions I and II moves downward to the right as cohesion increases (b). The failure criterion seems to rotate clockwise as critical failure ratio increases (c).

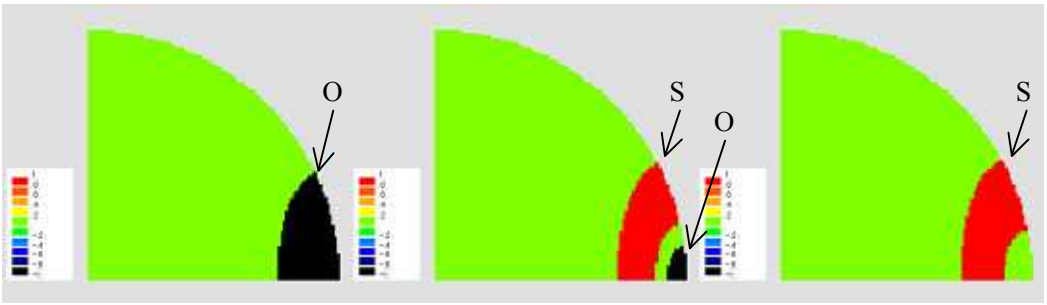

(a) A in figure 7a (b) B in Figure 7a (c) C in Figure 7a

Figure 8. Failure mode of weakness planes on the Schmidt net. O and S denote the opening and slip, respectively. Plane failures were all in the opening in (a), the opening and slip in (b) and all in the slip in (c).

6 CONCLUDING REMARKS

The "weakness plane model" was developed to simulate the effects of various stress states on the strength of rocks. The model assumes numerous planes of weakness whose directions are uniformly distributed in a rock; each plane slips or opens based on the Coulomb criterion with a tension cut-off; and the rock is regarded as failed when the ratio of the failed plane number to that of all planes reaches a certain value. The same size and strength parameters were assigned to all planes and no complicated statistical functions were used. The model was applied to true triaxial compression, uniaxial tension, Brazilian and extension tests. The model is very simple but the effects of the stress state were simulated very well. Stress and plane failure distributions on the Schmidt net has increased the understanding of the mechanism of stress state effects on rock strength.

A precise approximation of the strength behavior of specific test results is possible in the future by adapting Hoek and Brown or other nonlinear failure criteria for weakness planes, weighting the effects of tensile and shear failures of weakness planes on rock failure, assuming a non-uniform direction distribution for the planes of weakness, etc..

REFERENCES

Brace, W.F. 1964. Brittle fracture of rocks. In W.R. Judd (ed.), *State of Stress in the Earth's Crust*: 111-180. New York: American Elsevier.

Fujii, Y. & Uehara, Y. 2006. A study on deformation and behavior of rock subjected to axial extension under confining pressure. *J. MMIJ.* 122(6/7): 330-337. (in Japanese)

Koide, H., Takahashi, M., Kinoshita, S., Ishijima, Y. & Nakamura, A. 1986. Effects of Griffith cracks and inclusions on fracture criteria under a general triaxial state, *J. Mat. Sci. Japan* 35(392): 14-19. (in Japanese)

Mogi, K. (1967). Effect of the intermediate principal stress on rock failure. *J. Geophys. Res*. 72: 5117-5131.

Oikawa, Y. &. Yamaguchi, T. 2000. Tension test of granite under confining pressure. *Proc. MMIJ Annual Meeting* I: 175-176. (in Japanese)

Ramsey, J.M. & Chester, F.M. 2004. Hybrid fracture and the transition from extension fracture to shear fracture. *Nature* 428: 63-66.

Takahashi, T., Takahashi, M., Kiyama, T. & Takemura, T. 2009. A triaxial compression and triaxial extension test of Kimachi sandstone. In I. Vrkljan (ed.), *Rock Engineering in Difficult Conditions - Soft Rocks and Karst*: 381-386. Leiden: CRC Press/Balkema.

Tani, K. 1996. Extension failure mechanism of homogeneous soft rock under low confining pressure. *Proc. 27th Symposium of Rock Mechanics, Japan*: 226-230. (in Japanese)

You, M. 2009. True-triaxial strength criteria for rock. *Int. J. Rock Mech. Min. Sci.* 46: 115-127.